Journal of Alloys and Compounds 495 (2010) 247–253

Contents lists available at ScienceDirect

Journal of Alloys and Compounds

journal homepage: www.elsevier.com/locate/jallcom

Persistent luminescence in rare earth ion-doped gadolinium oxysulfide phosphors

Bingfu Lei[a,b], Yingliang Liu[a,*], Junwen Zhang[a], Jianxin Meng[a], Shiqing Man[a], Shaozao Tan[a]

[a] Department of Chemistry, Jinan University, Guangzhou 510632, People's Republic of China
[b] Department of Physics, Jinan University, Guangzhou 510632, People's Republic of China

ARTICLE INFO

Article history:
Received 21 October 2009
Received in revised form 26 January 2010
Accepted 28 January 2010
Available online 6 February 2010

Keywords:
Rare earth ions
Gadolinium oxysulfide
Long afterglow

ABSTRACT

A series of rare-earth ion-doped gadolinium oxysulfide phosphors $Gd_2O_2S:RE^{3+}$, Ti, Mg (RE = Ce, Pr, Nd, Sm, Eu, Tb, Dy, Ho, Er, Tm, Yb) were synthesized by solid-state reaction. The excitation and photoluminescence spectra, afterglow spectra, afterglow decay curves and thermoluminescence spectra of the phosphors were examined. According to the afterglow spectra, gadolinium oxysulfide doped with rare-earth ions were classified into three groups. When rare earth ions such as Eu^{3+}, Sm^{3+}, Dy^{3+}, Ho^{3+}, Er^{3+} and Tm^{3+} were introduced into the Gd_2O_2S host, their characteristic emission as well as that from Gd_2O_2S:Ti, Mg were observed. In case of Yb^{3+} and Nd^{3+}, only the broadband luminescence of Gd_2O_2S:Ti, Mg was obtained. Gadolinium oxysulfide doped with Pr^{3+}, Tb^{3+} and Ce^{3+} did not show afterglow emission. The calculated trap energy levels of the samples were compared. The role of Ti and Mg ions and a potential mechanism for persistent luminescence in the samples were discussed.

1. Introduction

Afterglow phosphor is a kind of interesting materials that emitting long-lasting phosphorescence (LLP) for a long time after removal of the excitation source. These non-radioactive long afterglow phosphors are used increasingly in a range of fields such as emergency light sources, luminous paint, road signs, billboards, graphic arts and interior decoration. The first record of a LLP material which was found in nature is in the Song Dynasty of China (11th century A.D.) [1]. Around 1600, Galilei was attracted by the Stone of Bologna, which emits yellow to orange LLP when subjected to sunlight. Without knowing the physical processes, Galilei excluded mystery as the origin of that phenomenon. In 1671, by heating the mineral with carbon black, Kirchner was able to intensify the luminescence, indicating that impurity-type luminescence of BaS, not $BaSO_4$, is the origin of the LLP phenomenon [2,3]. For more than one century, sulfide-based phosphors, such as ZnS:Cu, have been in use as LLP phosphors and widely studied as luminescent host lattices [4–6]. However, these sulfide-based phosphors are not stable and theirs phosphorescence is not bright or long enough for applications. Radioisotopes have had to be added into this kind of phosphor in order to obtain the acceptable performance, but the use of radioisotopes has been restricted because of safety and environment considerations [7]. So there has been a great demand for new type host lattice substitutes in recent years.

In 1996, Matsuzawa et al. firstly reported the green and blue emitting LLP phenomenon from Eu^{2+}-doped alkaline earth aluminates [8]. Since then, oxide-based LLP materials, especially aluminate-base and silicate-base luminescent host lattices which can be used for glass components, have attracted more and more attention and have been developed rapidly to replace the conventional long-lasting phosphorescent materials [9–15]. The brightness and persistent time of these new phosphors are more than 10 times longer than that of the previous sulfides, and remain visible well over 10 h after UV excitation. At present, the performance of these aluminates-based afterglow phosphors, such as $SrAl_2O_4:Eu^{2+}$, Dy^{3+} (green), $CaAl_2O_4:Eu^{2+}$, Nd^{3+} (blue), already meet the requirement for practical applications [14,15]. However, the afterglow intensity and/or persistent time of the LLP phosphors emitting in the longer (orange to red) region is still far away from expected target. Therefore, researchers in this field are currently focusing on the preparation and properties of red and orange emitting afterglow phosphors.

Among the host lattices reported for luminescence materials, rare-earth oxysulfides (Ln_2O_2S, Ln = La, Gd, Y, Lu) activated with trivalent rare-earth ions have been extensively investigated because of their high luminescence efficiency. Certain members of this family are commonly used in commercial applications, such as Gd_2O_2S:Tb is used as an input phosphor in a commercial X-ray image intensifier tube and Y_2O_2S:Eu is used as the red phosphor in a color television tube [7,16]. According to the report of Murazaki in 1999, LLP phenomenon can be observed in $Y_2O_2S:Eu^{3+}$ phosphor and the properties can be greatly enhanced when co-doped with Mg and Ti ions [17]. This important founding has initiated

* Corresponding author. Tel.: +86 20 85221813; fax: +86 20 85221697.
E-mail address: tliuyl@jnu.edu.cn (Y. Liu).

0925-8388/$ – see front matter © 2010 Elsevier B.V. All rights reserved.
doi:10.1016/j.jallcom.2010.01.141

a lot of interesting in the LLP of this phosphor and its analogues [18–30]. It was reported that co-doping with Mg and especially Ti ions affected the phosphorescence of $Y_2O_2S:Eu^{3+}$ phosphor, and the Ti component can be substituted by Zr or Ta [17]. However, the role of the Ti ion is still uncertain. Traps responsible for the thermoluminescence are thought to play an important role in persistent afterglow emitting. For rare-earth oxysulfides it is still unknown which kind of defect is responsible for the LLP, therefore, systematic investigations on this kind of materials are required.

In general, Nd^{3+}, Ho^{3+}, Er^{3+}, Tm^{3+} and Yb^{3+} are mostly used as activator ions for infrared (IR) and upconversion luminescence materials [7,31,32]. In the present work, a series of Gd_2O_2S phosphors co-doped with rare-earth ions, Mg and Ti ions were prepared. Comparison of the persistent luminescence and thermoluminescence of these phosphors was carried out in detail. The effects of the Ti ions, traps which were responsible for the long-lasting phosphorescence and mechanism of persistent luminescence were discussed.

2. Experimental

RE^{3+}-doped (RE = Ce, Pr, Nd, Sm, Eu, Tb, Dy, Ho, Er, Tm, Yb) gadolinium oxysulfide phosphors were prepared by a flux fusion method with stoichiometric amounts of Gd_2O_3 (99.999%), S (99.99%), and rare earth oxides (4N) as the raw materials, using a binary flux composition (S and Na_2CO_3 (99.99%) in a ratio of 1:1 at 30 wt% of the total weight of the raw materials). A RE^{3+} dopant concentration of 5 mol% of that of Gd^{3+} was used. The TiO_2 and $Mg(OH)_2{\cdot}4MgCO_3{\cdot}6H_2O$ were added as Ti and Mg source, and the concentration of Ti and Mg ions were 2 and 4 at.% with respect to Y^{3+} ions, respectively. The raw materials were mixed and preheated at 400 °C for 2 h, then fired at 1050 °C for 6 h using alumina crucibles with alumina lids in a weak reducing atmosphere (CO gas produced by a kryptol furnace at high temperature). The raw product was obtained by subsequent quenching in air. After the firing process, the air cooled raw product was washed with 5% hydrochloric acid to remove any residual sulfur and flux byproducts. The raw product was washed with ultra-pure water several times until the pH was 7, washed with alcohol and then dried at 80 °C.

The phase identification of synthesized powder samples was carried out by a MSAL-XRD2 X-ray powder diffractometer using a Cu target radiation source (λ = 1.5405 Å) operating at 40 kV and 30 mA with a scanning step of 0.02° (2θ) and scanning speed of 4° (2θ)/min. The powder samples were mounted into a flat holder to minimize any eventual preferential orientation of the obtained samples. The routine X-ray powder diffraction analyses revealed that all of the samples contained only a single phase which closely matched that of the corresponding Gd_2O_2S standard (JCPDS card No. 26-1422). The phase analyses demonstrated that Gd_2O_2S is hexagonal with cell dimensions of a = 0.3852 nm and c = 0.6667 nm. From the XRD analyses, we can conclude that the rare earth ions substitute Gd^{3+} ions without disturbing the crystal lattice.

The photoluminescence spectra were measured by a VARIAN fluorescence spectrophotometer at room temperature equipped with a monochromator (resolution: 0.2 nm) and 150 W Xe lamp as the excitation source. The powder sample loaded on a holder provided by VARIAN was mounted about 45 °C to the excitation source for photoluminescence measurement. Suitable filters were used to correct for the baseline shift due to any stray light. The slit and PMT detector voltage were adjusted to allow for the detection of a strong signal without overloading the detector. For comparison of different samples, all samples were measured using the identical parameters of the spectrophotometer. The afterglow emission spectra of different samples at different times after turning off the excitation lamp and the afterglow intensity decay curves were measured on the same VARIAN fluorescence spectrophotometer. The excitation light from the Xe lamp attached on the spectrofluorometer was cut off after irradiating for 5 min to the samples, and then the afterglow emission spectra and decay curve were recorded immediately after such exposure. During the afterglow emission acquisition, the excitation source remained cut off and the emission from the sample was monitored using the kinetic analysis mode. The scan speed of the afterglow emission spectra was increased to 3600 nm/min in order to ensure the fact that the intensity change during the measurement was negligible.

Thermoluminescence (TL) measurements were performed by heating the irradiated sample using a TL meter (FJ-427A, Beijing Nuclear Instrument Factory). The samples were first excited for 5 min using a standard 254 nm UV radiation lamp with a power of 15 W. Then the radiation source was removed and the samples were heated at a linear rate of 2 K/s.

3. Results and discussion

3.1. The luminescence properties of rare earth ion-doped Gd_2O_2S phosphors

Fig. 1 shows the excitation and emission spectra of the $Gd_2O_2S:RE^{3+}$, Ti, Mg (RE = Eu, Sm, Dy, Ho, Er, Tm, Nd, Yb, Pr, Tb, Ce) phosphors, respectively. Inspection of these results reveals several key points. Firstly, a broad excitation band centered at about 260 nm, which is the characteristic absorption of the Gd_2O_2S:Ti, Mg

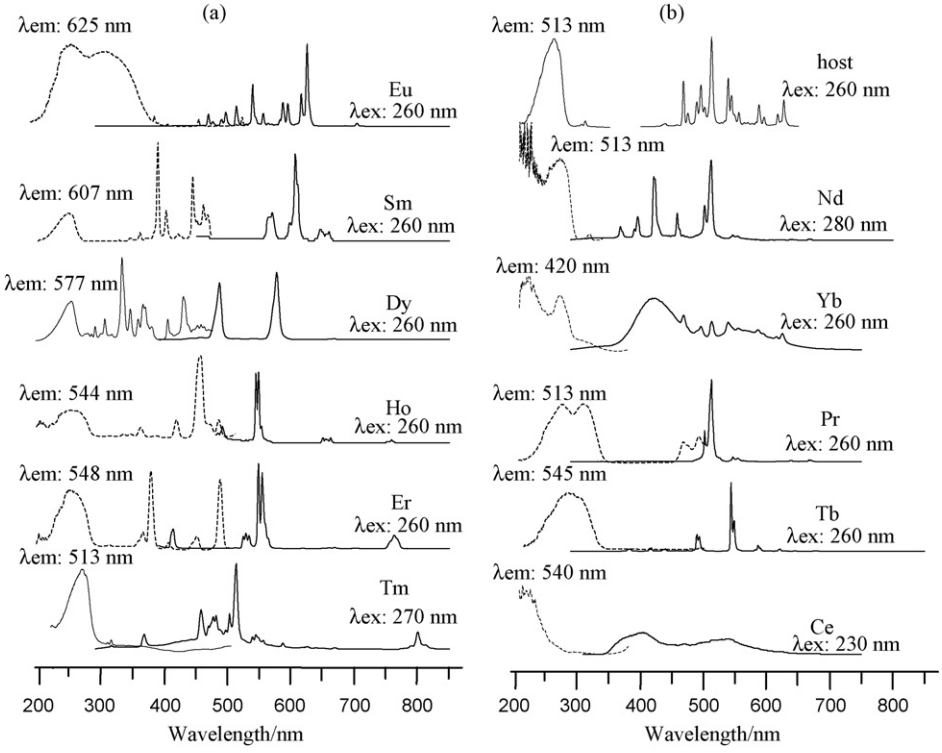

Fig. 1. Excitation spectra (dashed line) and emission spectra (solid line) of $Gd_2O_2S:RE^{3+}$, Ti, Mg phosphors. (a) RE = Eu, Sm, Dy, Ho, Er, Tm (b) RE= Nd, Yb, Pr, Tb, Ce.

sample as shown in Fig. 1(b), is exhibited in almost all the samples except for Ce^{3+}-doped one. The different excitation spectrum of Ce^{3+}-doped sample is associated with its special $[Xe]4f^1$ electronic configuration [33]. Under 230 nm excitation, two broad emission bands originated from transition between the excited states and the $^2F_{5/2}$ and $^2F_{7/2}$ states can be observed in the Ce^{3+}-doped sample, as shown in Fig. 1. Similar excitation spectrum is also observed in the Yb-doped sample. The broad excitation band of this sample can be assigned to the transition from the $^2F_{5/2}$ state of Yb^{3+} to the charge transfer state (CTS), and the broad emission band located at about 420 nm can be assigned to the transition between the CTS and the ground states [34].

Secondly, when rare earth ions such as Eu, Sm, Dy, Ho and Er are introduced into the Gd_2O_2S host lattice, their characteristic $f \rightarrow f$ transitions line excitation peaks can be observed besides the 260 nm broad band. Especially in the Gd_2O_2S:Eu, Ti, Mg sample, a strong excitation band caused by the $Eu^{3+} \rightarrow O^{2-}$ charge-transfer transition can be observed at about 330 nm [28]. Under excitation by the 260 nm host absorption or by the strongest $f \rightarrow f$ line transition, such as the 413 nm from $^6H_{5/2} \rightarrow {}^4L_{13/2}$ of Sm^{3+}, no difference can be observed in their emission spectra of these Eu, Sm, Dy, Ho or Er-doped phosphors, which indicating the occurrence of efficient energy transfer between the host to the rare earth ions [35]. The strongest emission peak located at 625 nm of Eu^{3+}-doped sample comes from the $^5D_0 \rightarrow {}^7F_2$ transition [28]. As for the Gd_2O_2S:Sm, Ti, Mg sample, three groups characteristic line peaks of Sm^{3+} located at 570, 607 and 646 nm, which are due to the transitions of $^4G_{5/2} \rightarrow {}^6H_{5/2,7/2,9/2}$, respectively [35]. The emission spectrum of Gd_2O_2S:Dy, Ti, Mg has two prominent emission groups located at 485 and 577 nm, which correspond to the transitions of $^4F_{9/2} \rightarrow {}^6H_{15/2}$ (blue) and $^4F_{9/2} \rightarrow {}^6H_{13/2}$ (yellow), respectively [36]. In the cases of Ho and Er-doped samples, green emission can be observed with sharp line emission peaks located at about 544 and 548 nm, which originate from the $^5S_2 \rightarrow {}^5I_8$ (Ho), and $^4S_{3/2} \rightarrow {}^4I_{15/2}$ (Er), respectively [32,37].

Thirdly, Gd_2O_2S:RE, Ti, Mg (RE = Tm, Nd) samples only exhibit very weak emission peaks in the visible region. However, under 260 nm excitation, sharp line emission peaks can be observed as shown in Fig. 1. These several emission peaks of Nd^{3+} or Tm^{3+}-doped samples is come from the trace impurities of Tb, Pr, which is confirmed by ICP analysis results of the Gd_2O_3 raw materials. The Gd_2O_2S host lattice is very sensitive to Pr and Tb dopant [7,38], therefore, there are several sharp line emission in the host, as shown in the top part of Fig. 1(b). In the Pr and Tb-doped samples, the strong emission peaks located at 513 and 545 nm come from the $^3P_0 \rightarrow {}^3H_4$ (Pr^{3+}) and $^5D_4 \rightarrow {}^7F_5$ (Tb^{3+}), respectively [7,38].

3.2. The persistent luminescence of Gd_2O_2S:Ti, Mg

As shown in Fig. 2, the introduction of Ti ions into the Gd_2O_2S host caused an afterglow emission band centered at about 590 nm. The position and profile of this afterglow emission spectrum is consistent with that of Y_2O_2S:Ti previously reported [19,27]. The luminescence mechanism of the Y_2O_2S:Ti phosphor is thought to result from the recombination of Ti-related trap defects. It was thought that the donor and acceptor energy levels of the Y_2O_2S:Ti phosphor were controlled by the substitution of Ti^{4+} and/or Ti^{2+} ions for Y^{3+} ions, respectively [19,27]. However, the possibility of other processes cannot be excluded. Here, we speculate that the afterglow emission of Ln_2O_2S:Ti (Ln = Y, Gd) may result from two possibilities: (1) Ti ions may be reduced in the reducing atmosphere during sample synthetic process, as a consequence, coexistence of mixed valence states of Ti ions (Ti^{2+}, Ti^{3+} and Ti^{4+}) with different ratio in these samples are expected. Here, the afterglow emission located at 590 nm can be assigned to the transition of

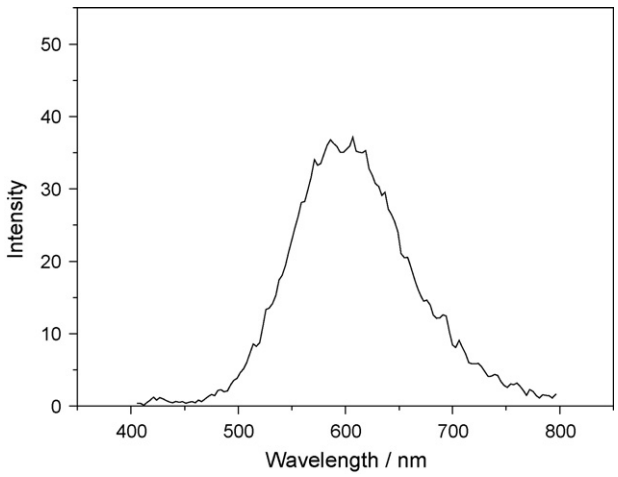

Fig. 2. The afterglow emission spectrum of Gd_2O_2S:Ti.

Ti^{3+} ($^2E \rightarrow {}^2T_2$), which is consistent with that of $CaGdAlO_4$:Ti^{3+} phosphor [39]. (2) The emission band could be caused by the recombination of electron and hole on Ti^{4+}, which is similar to the charge balance requirement due to the nonequivalent substitution of Gd^{3+} by the changeable valence Ti ions [19,27]. This process may occur in two steps: initially, Ti^{4+} captures one electron under UV light to form the excited Ti^{3+*} ion ($Ti^{4+} + e \rightarrow Ti^{3+*}$), which has a hole affinity, may then capture a hole which results in emission, $Ti^{3+*} + \text{hole} \rightarrow Ti^{4+} + h\nu$. It should be noted that the essential mechanism of the afterglow emission of Ln_2O_2S:Ti (Ln = Y, Gd) is still unclear because of the lack of specific data, as discussed later, however, it is certain that the emission band located at 590 nm plays an important role in the LLP of the rare earth ion-doped Ln_2O_2S phosphors [17,18,20,22,23,26].

The introduction of Mg co-dopant in to the Gd_2O_2S:Ti sample shows obvious enhancement of the 590 nm afterglow emission. As for the influence of Mg^{2+} in the Ti, Mg-co-doped sample, it was reported that the introduction of Mg^{2+} ions formed interstitial defect levels that favor the energy store and consequent long afterglow emission [40]. Another possibility is that the Mg^{2+} was used as charge compensator due to the different valence substitution between Ti, Mg^{2+} and Gd^{3+}. Therefore, the Mg^{2+} co-doping changed the inherent trap levels of the Ti single-doped sample and created new electronic donating and accepting levels between the host lattice band gap that was useful to absorb energy under excitation [24,27].

3.3. The LLP properties of Gd_2O_2S:RE^{3+}, Ti, Mg (RE = Ce, Pr, Nd, Sm, Eu, Tb, Dy, Ho, Er, Tm, Yb)

Figs. 3–5 shows the afterglow emission spectra of these Gd_2O_2S:RE^{3+}, Ti, Mg (RE = Ce, Pr, Nd, Sm, Eu, Tb, Dy, Ho, Er, Tm, Yb) phosphors. The emission intensities of Fig. 3 are normalized by its maximum intensity, respectively. As shown in Fig. 3, the afterglow spectra of the Gd_2O_2S:RE^{3+}, Ti, Mg (RE = Sm, Eu, Ho, Er, Tm, Dy) phosphors mostly contain a mixture of sharp line peaks and one broad band. The former can be attributed to the characteristic f–f transitions of these ions, and the latter belongs to the emission of the Ti ions, which is consistent with the above-mentioned photoluminescence results. It should be pointed out that some line-shape emission peaks originated from the electronic transitions of these rare earth ions are superimposed because the Ti related afterglow emission in Gd_2O_2S is relatively strong, for example of the Dy^{3+}-doped sample.

Fig. 4 presents the afterglow emission spectra of the Yb^{3+} and Nd^{3+}-doped samples. It is clear that there is no characteristic emis-

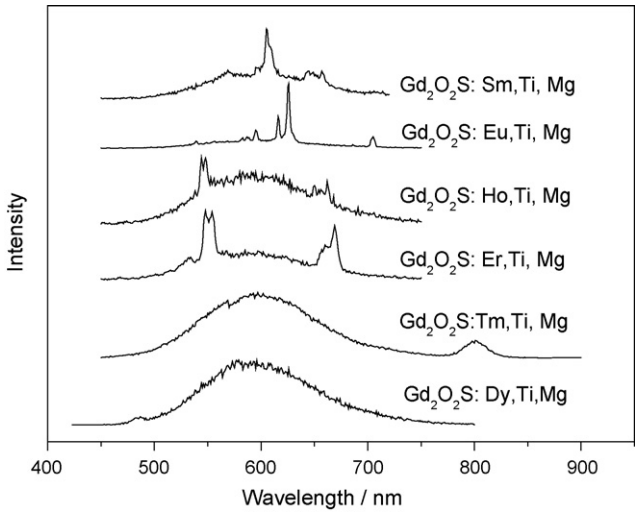

Fig. 3. Afterglow emission spectra of $Gd_2O_2S:RE^{3+}$, Ti, Mg (RE = Sm, Eu, Ho, Er, Tm, Dy).

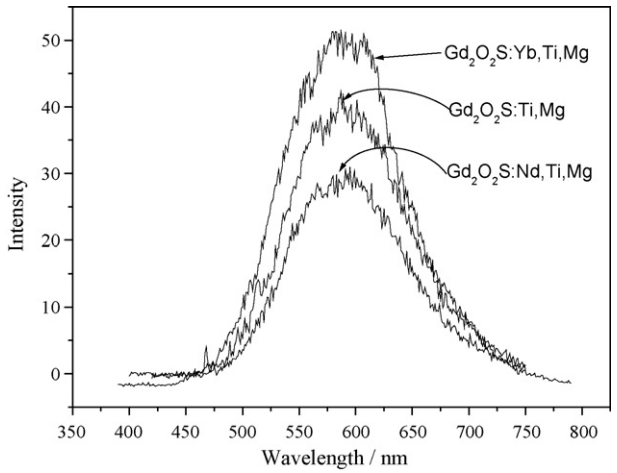

Fig. 4. Afterglow emission spectra of $Gd_2O_2S:RE^{3+}$, Ti, Mg (RE = Yb, Nd).

sion from Yb^{3+} or Nd^{3+} except for the broad band centered at 590 nm is observed in their afterglow emission spectra. This afterglow emission bands is identical to that of the Gd_2O_2S:Ti, Mg as mentioned above, so we conclude that the afterglow emission in

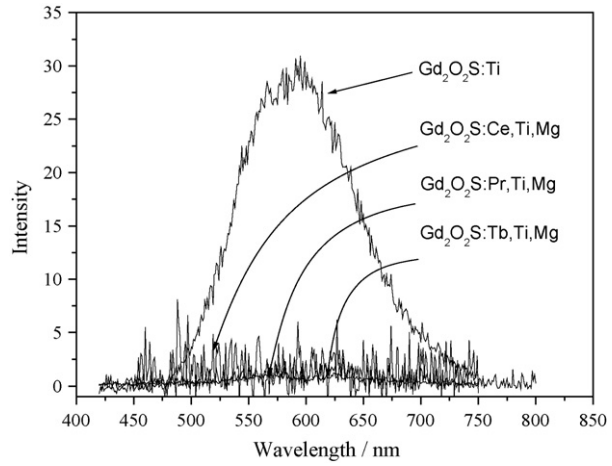

Fig. 5. Afterglow emission spectra of $Gd_2O_2S:RE^{3+}$, Ti, Mg (RE = Ce, Pr, Tb).

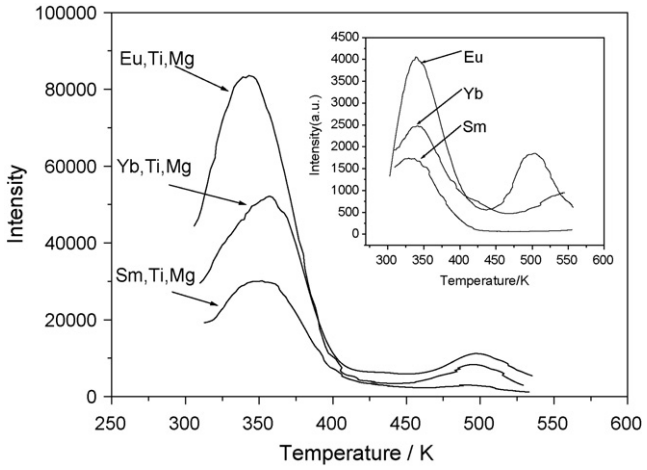

Fig. 6. The thermoluminescence spectra of RE^{3+} singly-doped and Ti, Mg co-doped $Gd_2O_2S:RE^{3+}$ phosphors (RE = Sm, Eu, Yb).

the Yb^{3+} and Nd^{3+}-doped samples can be ascribed to the emission of Ti ions.

In the cases of Ce^{3+}, Pr^{3+} and Tb^{3+}-doped Gd_2O_2S:Ti, Mg samples, their afterglow emission decrease quickly within only a few seconds so that almost no afterglow emission can be observed for these phosphors after removal of the UV-lamp excitation, as shown in Fig. 5.

3.4. Thermoluminescence of $Gd_2O_2S:RE^{3+}$, Ti, Mg (RE = Ce, Pr, Nd, Sm, Eu, Tb, Dy, Ho, Er, Tm, Yb)

To further understand the difference in the afterglow characteristics of $Gd_2O_2S:RE^{3+}$, Ti, Mg (RE^{3+} = Ce, Pr, Nd, Sm, Eu, Tb, Dy, Ho, Er, Tm, Yb) phosphors, we have examined the thermoluminescence spectra of all the $Gd_2O_2S:RE^{3+}$ and $Gd_2O_2S:RE^{3+}$, Ti, Mg phosphors in order to obtain some information about the influence of the traps created under UV irradiation on the afterglow properties. Figs. 6–8 shows the thermoluminescence spectra of these phosphors.

For the Sm^{3+}, Eu^{3+}, Yb^{3+}, Nd^{3+}, Dy^{3+}, Ho^{3+}, Er^{3+} and Tm^{3+}-doped phosphors, as shown in Figs. 6 and 7, respectively, one broad intense TL glow band is found between 300 and 400 K with a maximum at 350 K. However, for the Ce^{3+}, Pr^{3+} and Tb^{3+}-doped phosphors no obvious glow peaks were observed (Fig. 8). Utilizing the peak-shape method and the usual general-order kinetics expressions, the depths of these traps in these phosphors can be calculated from the

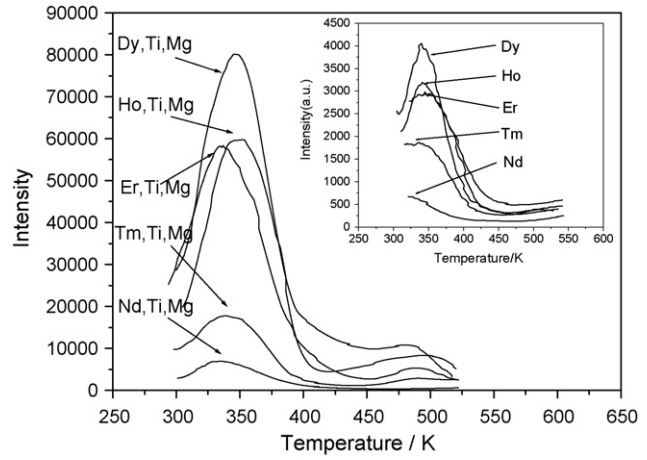

Fig. 7. The thermoluminescence spectra of RE^{3+} singly-doped and Ti, Mg co-doped $Gd_2O_2S:RE^{3+}$ phosphors (RE = Ho, Er, Tm, Dy, Nd).

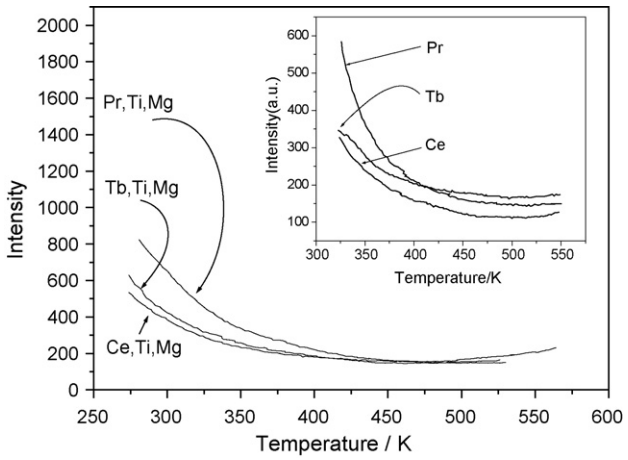

Fig. 8. The thermoluminescence spectra of RE^{3+} singly-doped and Ti, Mg co-doped $Gd_2O_2S:RE^{3+}$ phosphors (RE = Ce, Pr, Tb).

TL spectra by the following function [41–43]:

$$I(T) = sn_0 \exp = \left(-\frac{E_t}{\kappa_B T}\right) \times \left[\frac{(l-1)s}{\beta} \times \int_{T_0}^{T} \exp\left(-\frac{E_t}{\kappa_B T}\right) dT' + 1\right]^{-l/(l-1)} \quad (1)$$

where n_0 is the concentration of trapped charges at $t = 0$, κ_B is Boltzmann's constant, and β is the heating rate (2 K/s for our present experiment). The kinetics order l has a value 2 for the second-order process [42,43], and the frequency factor s is obtained by taking the derivative of Eq. (1) with respect to T and setting it to zero at the peak temperature (T_m). For a second-order mechanism, the trap depth E_t and n_0 are calculated by using the following equations [42,43]:

$$E = 305\left(\frac{\kappa_B T_m^2}{\omega}\right) - 2\kappa_B T_m \quad (2)$$

$$n_0 = \omega \times \frac{I_m}{\beta[2.52 + 10.2(\mu_g - 0.42)]} \quad (3)$$

where ω the full width at half maximum (fwhm), is known as the shape parameter and is defined as $\omega = \delta + \tau$, δ is the high-temperature half-width and τ is the low-temperature half width. The asymmetric glow peak shape is defined by the asymmetry parameters $\mu_g = \delta/\omega$. κ_B is Boltzmann's constant. T_m is the thermal peak temperature. I_m is the TL intensity at peak temperature T_m. Using the above-mentioned method and putting the measured values of T_m, ω, and κ_B into above equations, the trap depths (E_t) and n_0 are calculated and the results have been tabulated in Table 1. Due to the absence of TL glow peak in these Ce^{3+}, Pr^{3+}, Tb^{3+}-doped samples, their trap depths and densities were not available.

Table 1
Trap depths and densities of $Gd_2O_2S:RE^{3+}$ phosphors (RE = Ce, Pr, Nd, Sm, Eu, Tb, Dy, Ho, Er, Tm, Yb) with and without Ti, Mg co-dopants.

Dopant	E_t (eV)	n_0 (10^4)	Dopant	E_t (eV)	n_0 (10^4)
Eu	0.41	3.6	Eu, Ti, Mg	0.49	8.9
Yb	0.40	2.5	Yb, Ti, Mg	0.47	5.7
Sm	0.38	1.8	Sm, Ti, Mg	0.45	3.3
Dy	0.41	3.5	Dy, Ti, Mg	0.48	7.9
Ho	0.36	2.4	Ho, Ti, Mg	0.46	6.1
Er	0.40	2.3	Er, Ti, Mg	0.46	5.7
Tm	0.37	1.8	Tm, Ti, Mg	0.45	1.8
Nd	0.40	0.9	Nd, Ti, Mg	0.44	0.7

The trap depths of the glow peaks at a temperature of 350 K lie between 0.40 and 0.50 eV, which are suitable for LLP. From Table 1, it can be seen that the trap depths and densities of the singly-doped phosphors are smaller than those of the co-doped phosphors. Therefore, it may be concluded that the introduction of Ti ions increases the amount of defects. The trap depths greatly affect the duration of afterglow and the density of traps is responsible for the intensity of luminescence. This indicates that the co-doped phosphors should exhibit a longer afterglow than the singly-doped phosphors.

There are three possible types of trapping state in rare earth ion-doped oxysulfide [18–20,24,26,41]: (1) isoelectronic traps formed by ions which have a high electron (or hole) affinity, (2) charge traps formed by nonequivalent replacement of ions and (3) anion vacancies (sulfur or oxygen). When typical activators such as Eu^{3+} and Tb^{3+} were introduced into oxysulfide hosts, isoelectronic traps created by the replacement of Ln^{3+} constituent is regarded [44]. Due to the different ionization energies ($M^{2+}-M^{3+}$ and $M^{3+}-M^{4+}$) of Eu^{3+} and Tb^{3+} ions, different working models of the energy transfer process from the host to the activators have been proposed by authors [45,46]. The Eu^{3+} ion captures an electron first, while Tb^{3+} captures a hole first. Secondly, they capture the revise charge carrier, respectively, leading to the formation of 4f excited states. Based on this principle, the TL peaks at 350 K for the Sm^{3+}, Eu^{3+}, Yb^{3+}, Dy^{3+}, Nd^{3+}, Ho^{3+}, Er^{3+}, Tm^{3+} singly-doped phosphors may be ascribed to the isoelectronic traps formed by the substitution of Ln^{3+}. In the case of Ti ions-doped sample, it might be possible to introduce charge traps by replacing Ln^{3+} by the changeable valence Ti ions, as mentioned above. Therefore, it is expected that the capture of electrons by electron traps would give rise to the increased thermoluminescence. This process is demonstrated in the TL spectra in this study as shown in the Figs. 6–8: the intensities of thermoluminescence of the RE^{3+}(RE^{3+} = Sm^{3+}, Eu^{3+}, Yb^{3+}, Dy^{3+}, Nd^{3+}, Ho^{3+}, Er^{3+}, Tm^{3+}) and Ti co-doped phosphors are stronger than the RE^{3+}(RE^{3+} = Sm^{3+}, Eu^{3+}, Yb^{3+}, Dy^{3+}, Nd^{3+}, Ho^{3+}, Er^{3+}, Tm^{3+}) singly-doped phosphors. In the case of the Ce^{3+}, Pr^{3+} and Tb^{3+}-doped phosphors, there may be a reaction between the isoelectronic traps (holes) and the electron traps, which quenches the thermoluminescence. Based on these observations, it may be concluded that the persistent luminescence and thermoluminescence in these phosphors results from the traps formed by doping the oxysulfide with Ti, Mg ions and RE^{3+}.

3.5. The role of Ti ions in the LLP of $Gd_2O_2S:RE^{3+}$, Ti, Mg

Based on the above-mentioned results, it is clear that the addition of Ti ions greatly affects the luminescence intensity and the persistence time of the LLP in these rare-earth oxysulfide systems. The Ti ions are thought to have two roles in the process of LLP in $Gd_2O_2S:RE^{3+}$, Ti, Mg phosphors: producing suitable traps which are responsible for the persistent phosphorescence and energy transfer from the Ti ion to the RE^{3+} ion.

The $Gd_2O_2S:RE^{3+}$, Ti, Mg (RE^{3+} = Sm^{3+}, Eu^{3+}, Ho^{3+}, Er^{3+}, Tm^{3+}) phosphors, which exhibit characteristic emission in their afterglow spectra, show afterglow emission lasting for about 3 h, 5 h, 1.1 h, 1.2 h and 1.2 h, respectively. It is revealed that the decay times of the $Gd_2O_2S:RE^{3+}$, Ti, Mg (RE^{3+} = Ho^{3+}, Er^{3+}, Tm^{3+}) phosphors are consistent with that of Gd_2O_2S:Ti, Mg (1.5 h). As we know, the rare earth ions are thought to behave as activators in the persistent afterglow phosphors [47], so there is a possibility that energy transfer occurs from Ti to Ho^{3+}, Er^{3+} and Tm^{3+}. In our previous work, we proved the energy transfer process from Ti ions to Er^{3+} [37]. In the case of the Sm^{3+} and Eu^{3+}-doped phosphors, doping with Ti ions may produce suitable trap energy levels at room temperature which are useful for their afterglow emission.

It is well-known that these Ce^{3+}, Pr^{3+} and Tb^{3+} ions have $4f^1$, $4f^2$ and $4f^8$ electronic configurations, respectively. They readily lose

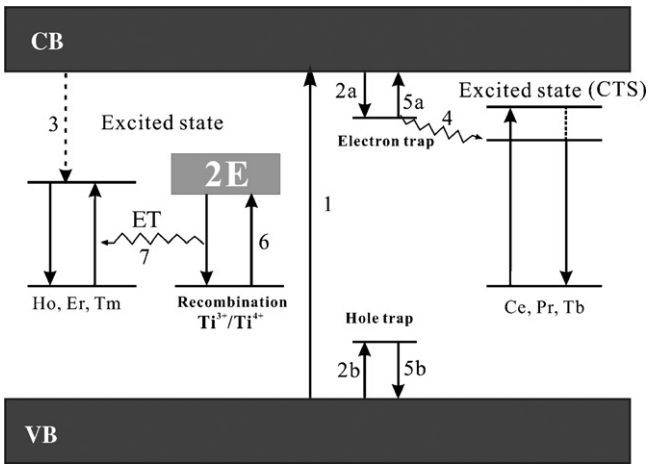

Fig. 9. The possible mechanism of long-lasting phosphorescence of Ti, Mg co-doped $Gd_2O_2S:RE^{3+}$ phosphors. ET = electron transfer, CTS = charge transfer state.

one electron to form empty or half-empty 4f electronic configurations, and this implies that these RE^{3+} ($RE^{3+} = Ce^{3+}$, Pr^{3+}, Tb^{3+}) have a tendency to be oxidized to the tetravalent state. This means that there is a possibility of electron-transfer quenching in these phosphors [16]. As reported previously [16], many rare earth ions show efficient luminescence in YVO_4, but the ions Ce^{3+}, Pr^{3+} and Tb^{3+} do not. This is because the quenching effect *via* a charge-transfer state ($RE^{4+} + V^{4+}$). In our oxysulfide samples, electron-transfer quenching may occur for the Ce^{3+}, Pr^{3+} and Tb^{3+} dopant ions through a charge-transfer state ($RE^{4+} + Ti^{3+}$). This electron-transfer quenching is reflected by their lack of afterglow emission and thermoluminescence as mentioned above. For these Yb^{3+} and Nd^{3+} ions, their low luminescent efficiency and relative stable valence results in the afterglow emission spectra that mostly exhibit the afterglow emission of Ti ions.

Overall, the role of Ti ions in the LLP of $Gd_2O_2S:RE^{3+}$, Ti, Mg system is complex and depends on the electronic configuration of the doped rare earth ion. For Sm^{3+} and Eu^{3+}, doping with Ti ions may produce a suitable trap energy level at room temperature for LLP. In the case of Ho^{3+}, Er^{3+} and Tm^{3+}, an energy transfer process from Ti to RE^{3+} exists. For Ce^{3+}, Pr^{3+} and Tb^{3+}, electron-transfer may quench the luminescence.

3.6. Possible mechanism of LLP in $Gd_2O_2S:RE^{3+}$, Ti, Mg phosphors

Phosphorescence or afterglow is related to the capture of energy by various types of traps and the subsequent release of this energy through emission. The persistence time of phosphorescence is determined by the number, nature and depth of the traps and by the efficiency of the trapping process. Although much work has been done on the Y_2O_2S:Eu, Ti, Mg long-lasting phosphor, until now there has not been a convincing mechanism proposed to explain the persistent luminescence in rare-earth oxysulfide systems. This is because of the complexity of the role of Ti and the differences between the various rare earth ions. Here, a new mechanism explaining the persistent luminescence in a gadolinium oxysulfide host is proposed based on the above-mentioned results. An illustration showing the complex luminescence and afterglow processes of Gd_2O_2S:RE, Ti, Mg phosphors is shown in Fig. 9.

Initially, UV-light exposure causes an electronic transition from the ground state of the RE^{3+} to the excited state (step 1), simultaneously electrons and holes are created in the host. For Sm^{3+} and Eu^{3+}, after excitation some electrons and holes can be stored in the electron traps or hole traps through a relaxation process (steps 2a and 2b). For Ho^{3+}, Er^{3+}, Tm^{3+}, Yb^{3+}, Dy^{3+} and Nd^{3+}, the excited electrons rapidly relax back to the ground state resulting in fluorescence emission (step 3). In the case of Ce^{3+}, Pr^{3+} and Tb^{3+}, a charge-transfer process ($Re^{4+} + Ti^{3+}$) may occur which quenches the luminescence (step 4). As the electrons and holes captured within the trap energy levels of Sm^{3+} and Eu^{3+}-doped phosphors are re-stimulated (steps 5a and 5b), some of them return to the excited state of the rare earth ion, resulting in characteristic f–f persistent afterglow emission as these electrons relax to the ground state. Some of the electrons may be captured by Ti^{4+} to form Ti^{3+*}, which has a hole affinity, may capture a hole which results in emission, $Ti^{3+*} + \text{hole} \rightarrow Ti^{4+} + hv$ (step 6). Taking into account the afterglow emission of Ho^{3+}, Er^{3+} and Tm^{3+}, it is assumed that a slow energy transfer process (step 7) occurs from Ti to Ho^{3+}, Er^{3+} and Tm^{3+}.

Significantly, this mechanism could explain the origin of the persistent luminescence in $Gd_2O_2S:RE^{3+}$, Ti, Mg phosphors. However, some questions still remain about the luminescent process of the Ti ion and the energy transfer process between Ti and some rare earth ions, further research is still under performing.

4. Conclusions

A series of rare earth ion-doped $Gd_2O_2S:RE^{3+}$, Ti, Mg (RE = Ce, Pr, Nd, Sm, Eu, Tb, Dy, Ho, Er, Tm, Yb) phosphors have been prepared by a conventional high-temperature solid-state method. The rare earth ion dopants were assigned to different categories according to their electron configuration and afterglow spectra. Trapping depths and concentrations were evaluated using a TL spectra. The defects in these phosphors and the role of the Ti and Mg ions in $Gd_2O_2S:RE^{3+}$, Ti, Mg phosphors were discussed, and a new model for explaining the luminescence and afterglow processes has been presented.

Acknowledgments

This work was supported by the National Natural Science Foundation of China (Grant Nos. 50872045, 20671042 and 30670523) and the Natural Science Foundation of the Guangdong Province (Grant Nos. 7005918, 05200555 and 2006B14801003).

References

[1] E.N. Harvey, A History of Luminescence, American Philosophical Society, PA, 1957, p. 18.
[2] E. Gubelin, International World of Gemstones, ABC-Verlag, Zurich, 1974.
[3] C. Feldmann, T. Justel, C.R. Ronda, P.J. Schmidt, Adv. Funct. Mater. 13 (2003) 511.
[4] Y. Kojima, T. Toyama, J. Alloys Compd. 475 (2009) 524.
[5] M. Fang, H. Wang, X. Tan, B. Cheng, L. Zhang, Z. Xiao, J. Alloys Compd. 457 (2008) 413.
[6] S.S. Pitale, S.K. Sharma, R.N. Dubey, M.S. Qureshi, M.M. Malik, Opt. Mater. 32 (2010) 461.
[7] S. Shionoya, W.M. Yen, Phosphor Handbook, CRC Press, Boca Raton, FL, 1999.
[8] T. Matsuzawa, Y. Aoki, N. Takeuchi, Y. Murayama, J. Electrochem. Soc. 143 (1996) 2670.
[9] S. Yao, Y. Li, L. Xue, Y. Yan, J. Alloys Compd. 490 (2010) 200.
[10] T. Li, M. Shen, L. Fang, F. Zheng, X. Wu, J. Alloys Compd. 474 (2009) 330.
[11] H. Wu, Y. Hu, Y. Wang, B. Zeng, Z. Mou, L. Deng, W. Xie, J. Alloys Compd. 486 (2009) 549.
[12] R. Wei, Z. Ju, J. Ma, D. Zhang, Z. Zang, W. Liu, J. Alloys Compd. 486 (2009) L17.
[13] C. Chang, W. Li, X. Huang, Z. Wang, X. Chen, X. Qian, R. Guo, Y. Ding, D. Mao, J. Lumin. 130 (2010) 347.
[14] X. Chen, C. Ma, X. Li, C. Shi, X. Li, D. Lu, J. Phys. Chem. C 113 (2009) 2685.
[15] J. Chen, F. Gu, C. Li, Cryst. Growth Des. 8 (2009) 3175.
[16] G. Blasse, B.C. Grabmaier, Luminescence Materials, Springer-Verlag, Berlin, 1994.
[17] Y. Murazaki, K. Arak, K. Ichinomiya, Rare Earths Jpn. 35 (1999) 41.
[18] B.F. Lei, Y.L. Liu, T. Gong, Z. Ye, C. Shi, Chem. J. Chin. Univ. 24 (2003) 782.
[19] P. Zhang, Z. Hong, M. Wang, X. Fang, G. Qian, Z. Wang, J. Lumin. 113 (2005) 89.
[20] L. Wang, L. Zhang, Y. Huang, D. Jia, J. Lu, J. Lumin. 129 (2009) 1032.
[21] A.N. Georgobiani, A.A. Bogatyreva, V.M. Ishchenko, O.Ya. Manashirov, V.B. Gutan, S.V. Semendyaev, Inorg. Mater. 43 (2007) 1073.
[22] G. Qiu, H. Wang, Y. Chen, X. Geng, Y. Yang, S. Shi, Z. Shi, J. Rare Earths 25 (2007) 104.

[23] Y. Wang, Z. Wang, J. Rare Earths 24 (2006) 25.
[24] Y. Chen, G. Qiu, X. Geng, Y. Yang, S. Shi, H. Wang, Z. Zhang, J. Rare Earths 25 (2007) 113.
[25] P.A. Rodnyi, Opt. Spectrosc. 107 (2009) 270.
[26] Z. Hong, P. Zhang, X. Fan, M. Wang, J. Lumin. 124 (2007) 127.
[27] P. Zhang, Z. Hong, H. Shen, Z. Xu, X. Fan, J. Rare Earths 24 (2006) 115.
[28] S. Mao, Q. Liu, M. Gu, D. Mao, C. Chang, J. Alloys Compd. 465 (2008) 367.
[29] S. Yuan, Y. Yang, B. Fang, G. Chen, Opt. Mater. 30 (2007) 535.
[30] T. Hang, Q. Liu, D. Mao, C. Chang, Mater. Chem. Phys. 107 (2008) 142.
[31] J.C. Boyer, F. Vetrone, J.A. Capobianco, A. Speghini, M. Zambelli, M. Bettinelli, J. Lumin. 106 (2004) 263.
[32] K.S. Lim, P. Babu, S. Lee, V. Pham, D.S. Hamilton, J. Lumin. 102–103 (2003) 737.
[33] J. Zhao, C. Guo, R. Guo, J. Hu, J. Alloys Compd. 436 (2007) 174.
[34] L. van Pieterson, M. Heeroma, E. de Heer, A. Meijerink, J. Lumin. 91 (2000) 177.
[35] B. Lei, Y. Liu, G. Tang, Z. Ye, C. Shi, Mater. Chem. Phys. 87 (2004) 227.
[36] Y. Liu, B. Lei, C. Shi, Chem. Mater. 17 (2005) 2108.
[37] J.W. Zhang, Y.L. Liu, S.Q. Man, J. Lumin. 117 (2006) 141.
[38] B. Liu, C. Shi, Z. Qi, J. Phys. Chem. Solids 67 (2006) 1674.
[39] N. Kodama, M. Yamaga, Phys. Rev. B 57 (1998) 811.
[40] M. Mikami, A. Oshiyama, Phys. Rev. B 60 (1999) 1707.
[41] S. Chatterjee, V. Shanker, H. Chander, Mater. Chem. Phys. 80 (2003) 719.
[42] B. Lei, B. Li, H. Zhang, L. Zhang, Y. Cong, W. Li, J. Electrochem. Soc. 154 (2007) H623.
[43] R. Chen, Y. Kirsh, Analysis of Thermally Stimulated Processes, Pergamon, Oxford, 1981, p. 159.
[44] T. Kano, J. Lumin. 29 (1984) 177.
[45] L. Ozawa, J. Electrochem. Soc. 124 (1977) 413.
[46] H. Yamamoto, T. Kano, J. Electrochem. Soc. 126 (1979) 305.
[47] C. Guo, C. Zhang, Y. Lu, Q. Tang, Q. Su, Phys. Stat. Sol. A: Appl. Res. 201 (2004) 1588.